α resonance structure in ^{11}B studied via resonant scattering of ^{7}Li+α

H. Yamaguchi,* T. Hashimoto, S. Hayakawa, D. N. Binh, D. Kahl, and S. Kubono
Center for Nuclear Study, University of Tokyo, RIKEN Campus, 2-1 Hirosawa, Wako, Saitama 351-0198, Japan

Y. Wakabayashi
Advanced Science Research Center, Japan Atomic Energy Agency, Tokai, Ibaraki, 319-1195, Japan

T. Kawabata
Department of Physics, Kyoto University, Kita-Shirakawa, Kyoto 606-8502, Japan

T. Teranishi
Department of Physics, Kyushu University, 6-10-1 Hakozaki, Fukuoka 812-8581, Japan
(Received 28 December 2010; published 8 March 2011)

A new measurement of α resonant scattering on ^{7}Li was performed over the excitation energy of 10.2–13.0 MeV in ^{11}B at the low-energy RI beam facility CNS Radioactive Ion Beam separator (CRIB) of the Center for Nuclear Study (CNS), University of Tokyo. The excitation function of ^{7}Li+ α at 180° in the center-of-mass system was successfully measured for the first time with the inverse kinematics method, providing important information on the α cluster structure in ^{11}B and the reaction rate of ^{7}Li(α,γ), which is relevant to the ^{11}B production in the ν process in core-collapse supernovae. The excitation function of the ^{7}Li(α,p) reaction cross section for 11.7–13.1 MeV was also measured.

DOI: 10.1103/PhysRevC.83.034306 PACS number(s): 25.55.−e, 21.60.Gx, 24.30.−v, 27.20.+n

I. INTRODUCTION

The exotic cluster structures in ^{11}B and ^{11}C have attracted much attention in recent years [1]. The $3/2^{-}_{3}$ state in ^{11}B at $E_{\rm ex} = 8.56$ MeV is regarded as a dilute cluster state [2], where two α particles and t are weakly interacting. In particular, the α cluster structure in ^{11}B was studied by measuring its isoscalar monopole and quadrupole strengths in the ^{11}B(d,d') reaction, and the 8.56-MeV state was suggested to have a dilute cluster structure [3,4]. A recent orthogonality-condition-model (OCM) calculation [5] proposed that the $3/2^{-}_{3}$ state near the α-decay threshold in ^{11}B (^{11}C) has a $2\alpha + t$ ($2\alpha + {}^{3}$He) dilute cluster structure, but the two α particles are not fully condensed into the lowest s orbit, unlike the three α particles in the Hoyle state [2]. According to the OCM calculation, a fully developed, cluster-condensed state emerges near the $2\alpha + t$ ($2\alpha + {}^{3}$He) decay threshold with a spin-parity of $1/2^{+}$ and isospin $T = 1/2$, but no corresponding state was reported in the nuclear-data compilations [6,7]. It is important to search for the unknown $1/2^{+}$ state and to clarify the cluster structure in ^{11}C and ^{11}B. A natural method to study the α cluster structure of ^{11}B is to form such a cluster state by the elastic scattering of ^{7}Li and α.

The ^{7}Li + α system is also related to the astrophysical reaction ^{7}Li$(\alpha,\gamma)^{11}$B. In the low-temperature stellar environment that ignites the p-p chains, ^{7}Li is destroyed via the ^{7}Li$(p,\alpha)^{4}$He reaction, and the ^{7}Li$(\alpha,\gamma)^{11}$B reaction is much weaker in comparison. However, in some high-temperature phenomena, the ^{7}Li$(\alpha,\gamma)^{11}$B reaction should play an important role. For example, in the ν process in core-collapse supernovae [8], ^{11}B is mainly produced via ^{4}He$(\nu,\nu'p)^{3}$H$(\alpha,\gamma)^{7}$Li$(\alpha,\gamma)^{11}$B, but the production can be enhanced with the ^{12}C$(\nu,\nu'p)^{11}$B and ^{12}C$(\overline{\nu_e}, e^{+}n)^{11}$B reactions. A precise comparison between the observed abundance ratio of ^{11}B/^{7}Li in stars and a calculation using the experimental ^{7}Li$(\alpha,\gamma)^{11}$B reaction rate may provide a constraint on the neutrino mixing parameter θ_{13}, as suggested in Ref. [8]. Resonance parameters, determined in the present study, allow for a precise determination of the ^{7}Li$(\alpha,\gamma)^{11}$B reaction rate at high temperature ($T_9 > 1$), giving a good insight on the roles of neutrino reactions and neutrino oscillation in the ν process.

In the present study, we measured the excitation function for excitation energy of $E_{\rm ex}$= 10–13 MeV in ^{11}B. The ^{7}Li$(\alpha,\gamma)^{11}$B reaction has been directly measured [9–12], but on resonances at lower energies. The excited states of ^{11}B in the current energy region of interest have been studied previously by ^{7}Li + α elastic scattering [13,14] or using other methods [9,15–22]; however, some of the resonance parameters are still uncertain. Among them, the α width Γ_α is an important parameter, as it reflects the α cluster structure of a state and also determines the magnitude of the (α,γ) and (α,p) reaction cross sections. However, it is not determined precisely for many resonances. Using inverse kinematics, the excitation function for the center-of-mass angles $\theta_{\rm cm}$ near 180°, where potential scattering is minimum and the resonances can be observed most clearly, was measured for the first time.

II. EXPERIMENTAL METHOD

A measurement of the ^{7}Li + α elastic scattering was performed at the CNS Radioactive Ion Beam (CRIB) facility [23,24] using the thick-target method in inverse kinematics [25]. The experimental setup is shown in Fig. 1. A ^{7}Li

*yamag@cns.s.u-tokyo.ac.jp

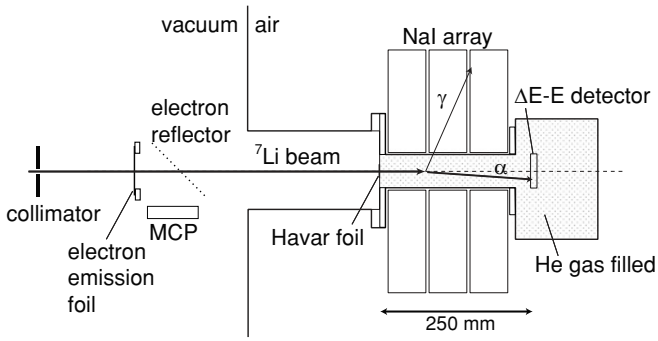

FIG. 1. Experimental setup of the measurement of ^{7}Li + α elastic scattering in inverse kinematics.

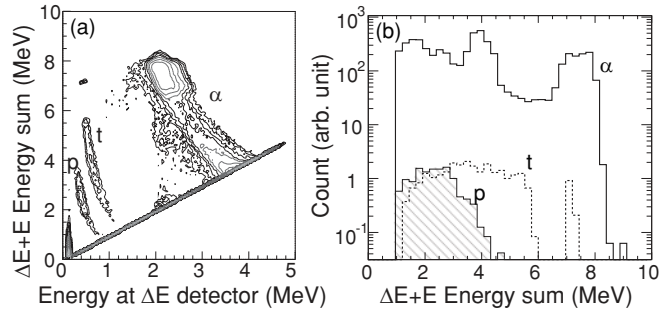

FIG. 2. (a) Two-dimensional energy plot for the ΔE-E detector for particle identification. (b) Energy spectra of α particles, protons, and tritons for >1 MeV.

beam was accelerated by the Azimuthally Varying Field (AVF) cyclotron of RIKEN and transported to the final focal plane (F3) of CRIB. The beam had a well-defined energy of 13.7 MeV and was collimated by a 3 × 3 mm^2 square aperture at F3. A microchannel plate (MCP) was used to measure the position and timing of the beam. A CsI-evaporated 0.7-μm-thick aluminum foil was placed on the beam axis for the secondary electron emission. The secondary electrons were reflected by 90° at a biased thin-wire reflector and detected at the MCP with a delay-line readout. The helium gas was housed in a 50-mm-diameter duct and a small target chamber. The helium gas was at 920 Torr and sealed with a thin (2.5-μm) Havar foil as a beam entrance window. α particles recoiling to the forward angles in the laboratory were detected by a ΔE-E detector, which consisted of 20-μm- and 480-μm-thick silicon detectors, placed directly in the gas chamber. The effective area of the detector was 20 cm^2. The silicon-strip detectors had a position sensitivity of 3 mm. The effective target length, namely, the distance from the beam entrance window to the detector, was 250 mm. To measure 478-keV γ rays from inelastic scattering to the first excited state of ^{7}Li, NaI detectors were placed around the duct. We used ten NaI crystals, each with a geometry of 50 × 50 × 100 mm^3. They covered 20%–60% of the total solid angle, depending on the reaction position in the target. The photopeak efficiency of the NaI detectors were measured at various positions in the gas target, using standard γ-ray sources. The measurement was successfully performed for 2.9 ×10^{10} ^{7}Li particles injected into the gas target over 60 h.

III. EXCITATION FUNCTIONS

A. Identification of α particles

The particle identification performed with the ΔE-E detector is shown as a two-dimensional energy plot in Fig. 2(a). As illustrated, α particles, protons, and tritons were clearly separated. Since the gas target was sufficiently thick to stop the ^{7}Li beam, particles heavier than lithium were not expected to reach the detector. Most of the particles measured were α particles from the elastic scattering, and only a small number of protons and tritons, which were possibly from ^{7}Li(α, p) reaction and from the breakup of ^{7}Li, were observed in the measurement, as compared in Fig. 2(b). α particles can be produced via the breakup of ^{7}Li. However, the number of such α particles should be of the same order as tritons, which were two orders of magnitude less than those from elastic scattering. They should give rise to a negligible source of α background in the elastic scattering spectra. The α particles in the beam as a form of contamination were also found to be negligible since very few particles having an energy above 1 MeV were detected for several hours when the target helium gas was changed to argon of an equivalent stopping power. As a result, we successfully performed a clean measurement of α particles resulting from ^{7}Li + α scattering.

B. Center-of-mass energy and its resolution

By performing kinematical calculations while considering the energy loss in the gas target, the measured energy of the α particle was converted to a center-of-mass energy for the ^{7}Li + α system ($E_{\rm cm}$). The incident angle of the collimated beam deviated within 0.5° of the beam axis. Therefore, the scattering angle in the laboratory frame $\theta_{\rm lab}$ (less than 10°) was known by the detection position at the ΔE-E detector.

The energy of the beam at any position in the gas target was obtained with a good precision (30–50 keV) based on direct energy measurements at various target pressures, which were compared with an energy loss calculation using the SRIM [26] code. The energy loss for recoiled α particles was also calculated with SRIM, using the same gas density. The energy-loss calculation appeared to be quite reliable because the higher edge of $E_{\rm cm}$ from the measured data was 4.4 MeV, which is in good agreement with $E_{\rm cm}$ expected from the beam energy at the beginning of the target.

Because of the thin dead layer between the two active components of the ΔE-E detector, shift and distortion appear in the energy spectrum around $E_{\rm cm}$ = 2.8 MeV. By measuring α and ^{7}Li particles at several fixed energies penetrating the dead layer, the thickness of the dead layer was determined to be about 0.8 μm. The helium gas in between the two silicon detectors also behaves as a dead layer with a thickness of the same order. In the present spectra, the shift and distortion effect was eliminated by making a correction based on a Monte Carlo simulation assuming this dead-layer thickness.

The overall uncertainty in $E_{\rm cm}$ was estimated as 50–100 keV, depending on the energy. The uncertainty mainly originated from the energy straggling of the ^{7}Li beam and α particles (40–70 keV), the energy resolution of the ΔE-E

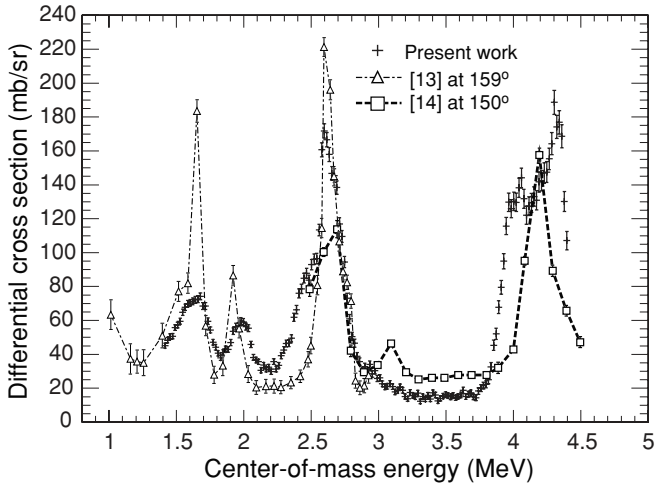

FIG. 3. Excitation function of ^{7}Li + α elastic scattering at around $\theta_{cm} = 170^\circ$. Previous measurements [13,14] are also shown.

detector (10–25 keV), and angular uncertainty due to the finite size of the detector (10–70 keV).

C. Excitation function of ^{7}Li + α elastic scattering

Figure 3 shows the excitation function of ^{7}Li + α elastic scattering cross sections obtained in this work, compared with previous measurements. In the present excitation function, a structure having peaks consistent with previous elastic scattering [13,14] and breakup [22] measurements was observed. The excitation functions shown in Fig. 3 were measured at different scattering angles, and it is not necessary that they coincide with each other. The present excitation function is for θ_{cm} 160°–180°, and the average θ_{cm} is 170°. No significant difference was seen in the spectrum when we selected events in a narrower angular range.

Compared with Cusson's result [13], our cross section at resonances appeared to be smaller, which may not be explained by the difference in the scattering angle. Our *R*-matrix calculation, which is described later, indicates that the maximum difference of the cross section between the cases of 150°–160° and 170° can be about 20 mb/sr, but only around high-spin resonances. The experimental resolution can account for the difference since our spectrum was broadened by the resolution of 100 keV at the lowest-energy points, while they were broadened by about 50 keV in Ref. [13]. The normalization in Ref. [13] was based on another measurement [27], and an uncertainty as much as 22% was assigned for the absolute cross section, which also may partly explain the difference. In the analysis of Ref. [13], the author had to assume a channel radius of 6.0 fm, which is unreasonably large for this system, possibly because of the overestimated cross section. In the other previous excitation function [14], the peak positions do not perfectly agree with our data, but the overall agreement is fairly good.

Compared with previous measurements, our measurements have more data points at smaller energy intervals due to our use of the thick target. Therefore, we can obtain more reliable information on resonant widths with our new measurement. Another advantage of the current method is that the systematic uncertainty from the long-time stability of the beam and detectors is small since we measured at all the energies simultaneously and a single counting of the beam particle was performed.

D. Inelastic scattering

Inelastic scattering events producing ^{7}Li at the first excited state were identified by measuring 478-keV γ rays with NaI detectors. In the energy spectrum of the γ rays [Fig. 4(a)], the peak at 478 keV was clearly observed. The excited ^{7}Li could be formed by inelastic scattering and fusion evaporation in the helium target. As shown in Fig. 4(b), the cross section for inelastic scattering, obtained by selecting α-γ coincidence events, was less than 1 mb/sr, two orders of magnitude smaller than the one for elastic scattering. Such a small

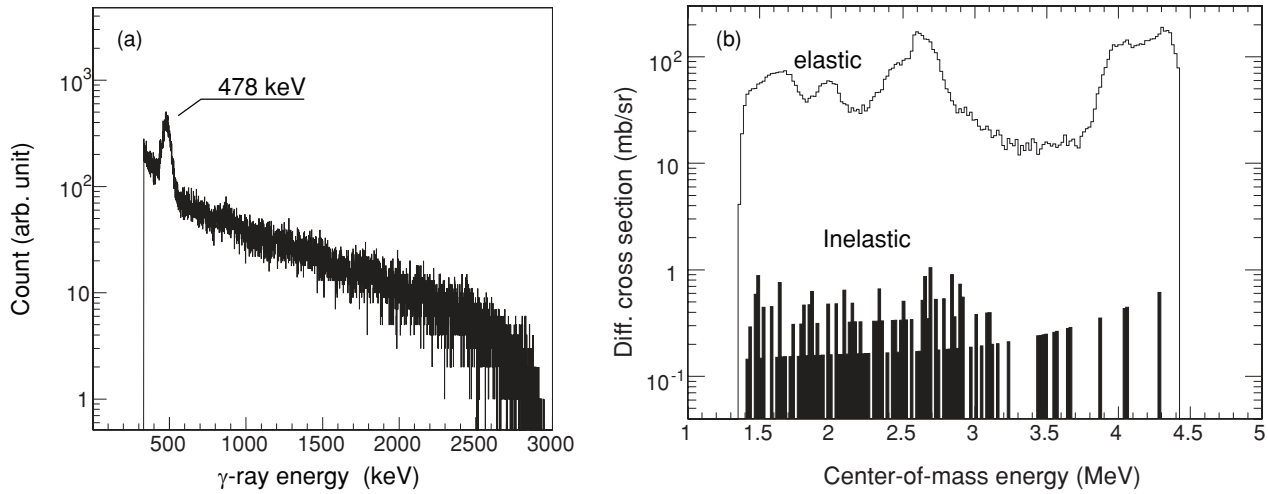

FIG. 4. (a) Energy spectrum of the γ rays for all measured events. (b) Excitation functions of ^{7}Li + α elastic scattering and inelastic scattering to the first excited state in ^{7}Li.

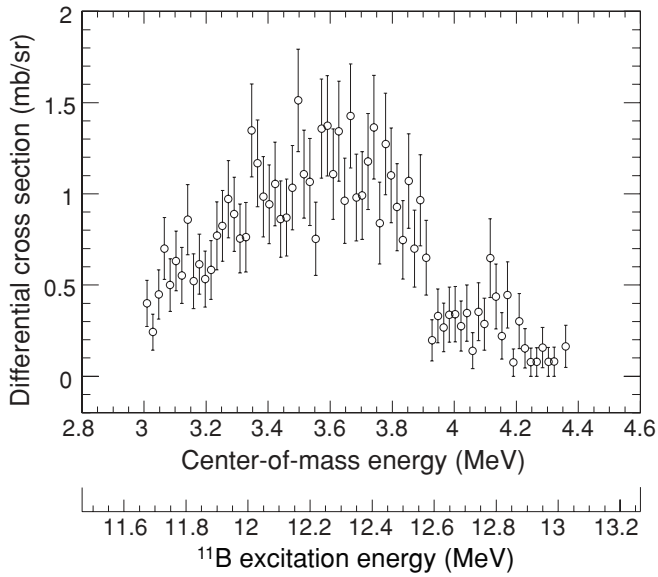

FIG. 5. Excitation function for the ^{7}Li$(\alpha, p)^{10}$Be reaction cross sections at $E_{\rm cm}$ = 3.0–4.4 MeV at $\theta_{\rm cm}$ of 165°–180°.

cross section appears to be in contradiction with the previous measurements, which obtained 5–15 mb/sr at $\theta_{\rm cm} = 150°$–160° for the same energy region [13,14]. We confirmed that the 478-keV γ-ray peak was not observed in the runs with argon target gas.

Several reasons that may explain the discrepancy are considered. The first reason is the reduction of the cross section at the large $\theta_{\rm cm}$. Cusson [13] claimed that pronounced minima were observed at $\theta_{\rm cm} = 60°$ and 120°. Assuming that the angular dependence could be extended with a similar phase, the next minimum is expected at around 180°, which corresponds to our measurement. Another possible reason is an accidental enhancement of the cross section at large $\theta_{\rm cm}$ by background events. In the normal kinematics measurements, the inelastic cross section at large $\theta_{\rm cm}$ was determined by counting ^{7}Li at forward angles. Kinematical calculations show elastically scattered α particles should also be detected at the same detector position, with a similar energy to ^{7}Li. With the single detector used in Ref. [13], these particles should not be subtracted clearly, as mentioned there. In the other measurement [14], particle identification was performed by a ΔE-E detector set, but single counters were used at small angles to separate elastically scattered particles from different target constituents. It might be possible that at $\theta_{\rm cm} = 150°$ the ΔE-E information could not be used to identify ^{7}Li clearly from α particles or other particles from the target. The normalization problem in Ref. [13] mentioned above could cause the enhancement of their cross section as well.

E. ^{7}Li(α, p) reaction

We selected proton events and obtained an excitation function for the ^{7}Li$(\alpha, p)^{10}$Be reaction cross sections, as shown in Fig. 5, assuming that the protons were predominantly from the ^{7}Li(α, p) reaction. As we observed no peaks in the γ-ray spectrum corresponding to the excitation energies in ^{10}Be, the reaction should be mostly to the ground state of ^{10}Be. The excitation function is for $E_{\rm cm} = 3.0$–4.4 MeV ($E_{\rm ex} = 11.7$–13.1 MeV), 0.5–2 MeV above the proton channel threshold at $E_{\rm ex} = 11.23$ MeV, and at $\theta_{\rm cm}$ of 165°–180°. No previous measurement in such a low-energy region is known. A previous measurement [28] used α beams having energies of 13–15 MeV, corresponding to $E_{\rm cm}$ about 9 MeV, and yielded a cross section of 0.5 mb/sr at $\theta_{\rm cm} = 170°$, comparable with our result.

IV. *R*-MATRIX ANALYSIS OF THE EXCITATION FUNCTION

As shown above, a structure with several peaks were clearly observed in the measured excitation function of ^{7}Li + α elastic scattering. We performed an analysis using an R-matrix calculation code (SAMMY-M6 [29]) to deduce resonance parameters. Initially, we calculated the excitation function assuming six α resonances (at 10.24, 10.34, 10.69, 11.29, 12.63, and 13.03 MeV), as shown in Table I. The energy, spin, and parity J^{π} of each resonance were fixed to the known values [6], and the width Γ_{α} was taken as a free parameter. The proton channel opens for the highest two resonances; however, the penetrability for the p decay is still small compared to the α decay, and no strong resonances corresponding to these two resonances were observed in the ^{7}Li(α, p) spectrum. Therefore, the resonances are assumed to be described mainly by Γ_{α}, and the width for the proton decay channel was not included in the calculation. For the excitation energies, the values from previous ^{7}Li + α measurement, among other reactions, were used. For some states the energies were determined more precisely by other reactions but were basically consistent with the values obtained by the previous ^{7}Li + α measurements. The energy broadening due to the experimental resolution was considered in the R-matrix calculations. There are two major discrepancies that could not be explained in the six-resonance calculation. The first one is a small bump seen around 11.1 MeV on the shoulder of the peak at 11.29 MeV. The second one is at 11.5–12.5 MeV, where the measured cross section was significantly less than the calculation. By introducing two resonances at 11.06 and 11.59 MeV, corresponding to the discrepancies, a best fit was obtained, as shown in Fig. 6. The resonance energies were also determined by the R matrix fit for these two resonances. A calculation with the same parameters but without the two newly introduced resonances is also shown in Fig. 6 for comparison.

We deviated the channel radius R_c within a range of 3–5 fm, and the calculation was best performed with $R_c = 3.2$ fm, which might be a rather small value for this system. However, a similar radius was used for an optical model calculation [30]. Larger channel radii resulted in less satisfactory fit results, as shown in Fig. 6 for the case of $R_c = 4.0$ fm. We investigated the channel-radius dependence of the calculated excitation function within the range, and the primary difference appeared as a shift of the baseline of the cross section, while the resonant peak heights are almost conserved for the same Γ_{α}. Considering this feature and that the baseline could be shifted by reasons such as interference from other

TABLE I. Best-fit resonance parameters of ^{11}B determined by the present work. The E_{ex} and J^{π} values shown in italics are from Refs. [6,7], and the other values are determined by our measurement.

E_{ex} (MeV)	J^{π}	l	Γ_{α} (keV)		Γ_w (keV)	γ_{α}^2 (MeV)		
			This study	Ref. [18]		This study	Ref. [9]	Ref. [13]
10.24	$3/2^-$	2	4 (<9)		72	0.089	0.227	0.05
10.34	$5/2^-$	2	19 ± 4		94	0.32		0.09
10.60	$7/2^+$	3	10 ± 3	30	15	1.1	0.640	0.084
11.06 ± 0.04	$5/2^+$ ($3/2^+$, $7/2^+$, $9/2^+$)	3	32 ± 20		41	1.25		
11.29	$9/2^+$	3	35 ± 4		63	0.89		
(11.59)[a]	($7/2^-$)	4	270 ($\Gamma_n = 580$)		(7)			
12.63 ± 0.04	($3/2^+$ [6], $5/2^+$, $7/2^+$, $9/2^+$ [22])[b]	3	33–400[c]	275	330	0.20–1.3		
13.03	$9/2^-$	4	$140\ ^{-80}_{+110}$		58	2.5		

[a]The values $3/2^+$ and $9/2^+$ were suggested in previous studies, while four spins are possible from our measurements alone.
[b]This resonance should not be regarded as a single-state resonance.
[c]Depends on J. See also Table II.

unaccounted resonances, the curve shown for $R_c = 4.0$ fm may underestimate Γ_{α} since the data could be fitted at the peaks but not at valleys. Hence, we adopted $R_c = 3.2$ fm, for which the whole shape of the peaks were reproduced perfectly, for the deduction of Γ_{α}.

The best-fit parameters are summarized in Table I. Here the Wigner limit Γ_w was calculated for an interaction radius $R = 3.2$ fm, and γ_{α}^2 was calculated by $\Gamma_{\alpha}/2P$, where P is the penetration factor. The Γ_{α} are only partially known in previous measurements. We compared Γ_{α} with the R-matrix analysis parameters in Ref. [18] and γ_{α}^2 with Refs. [9] and [13], in which Γ_{α} was not presented explicitly. As for γ_{α}^2, the agreement is not very good between the present work ($R = 3.2$ fm) and previous results ($R = 4.9$ fm [9] and $R = 6.0$ fm [13]), partly because they use different R to explain their data. Our measurement

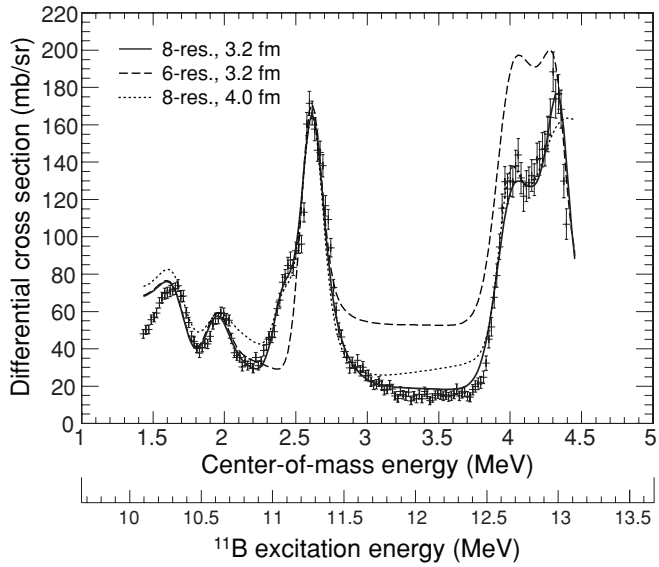

FIG. 6. Excitation function of ^{7}Li + α elastic scattering cross section fitted by R-matrix calculation curves. The solid curve is the best fit with $R_c = 3.2$ fm, and the dashed curve shows the same calculation without the two newly introduced resonances. The dotted curve is the best fit for $R_c = 4.0$ fm.

is considered to be quite insensitive to the total width, which includes other channel widths, since the spectral widths of all the resonances are mostly determined by the experimental resolution and Γ_{α}. Below we discuss each resonance in detail.

A. Resonances at 10.24 and 10.34 MeV

These lowest two resonances are known to be closely spaced. The peak was reproduced well by the R-matrix calculation by adjusting the width of the 10.34-MeV resonance. The calculation is not very sensitive to the width of the 10.24-MeV state, possibly due to the limited experimental energy resolution. The deviation at the lowest energy (around $E_{ex} = 10.2$ MeV) cannot be eliminated by varying widths of these resonances. The introduction of resonances at lower energies might be necessary to explain this deviation.

B. Resonances at 10.60, 11.06, and 11.29 MeV

In this energy region we observed two distinct peaks. The central energies of these two peaks are consistent with the known values of 10.60 and 11.29 MeV. A small bump was seen in the middle of the two peaks, and the discrepancy between the data and the calculated curve with only the two resonances is significantly large (see dashed curve in Fig. 6). We introduced an f-wave resonance at 11.06 MeV to eliminate the discrepancy, which could not be explained with the two known resonances. The best fit was obtained for $J^{\pi} = 5/2^+$, but other J^{π} ($3/2^+$, $7/2^+$, $9/2^+$) could not be excluded. Calculations with any other angular momentum significantly deviate from the measurement.

C. 11.5–12.5 MeV

The measured cross section in this region is flat and small, and it could not be reproduced by an R-matrix calculation with any simple α-decay channel resonance. This small cross section can be explained if there is a large probability of decaying to another channel, such as the neutron channel,

which opens at $E_{ex} = 11.45$ MeV. Thus, a broad resonance at $E_{ex} = 11.6$ MeV having a large neutron width, which is not known from previous works, was introduced. This assumption is quite artificial and may not imply the existence of a true single resonance having a large width, which far exceeds the Wigner limit. Similarly, a broad neutron resonance at $E_{ex} = 11.79$ MeV was assumed in a previous work [16] to explain their data of the ^{10}B(n,α) reaction measurement.

D. Resonance at 12.63 MeV

A strong peak was observed around 12.6 MeV in the spectrum. We determined the resonance energy as 12.63 ± 0.04 MeV by the R-matrix fit, instead of using the energy from a previously measured resonance at 12.56 MeV. The state at 12.56 MeV was observed in previous measurements, and it was considered to have $J^\pi = 1/2^+$ and an isospin $T = 3/2$, being an analog of the ^{11}Be ground state. It was observed via ^{9}Be(^{3}He,p) [31], ^{11}B(^{3}He, ^{3}He) [32], and other reactions [6]. The $J^\pi = 1/2^+(3/2^+)$ was assigned by a measurement of the ^{10}Be$(p,\gamma)^{11}$B reaction [33]. In Ref. [33], they measured the angular distribution of γ rays and concluded that the distribution is consistent only with $J^\pi = 1/2^+$ or $3/2^+$, and the former is more likely. However, a $T = 3/2$ state is unexpected to be observed as a strong resonance via ^{7}Li + α scattering, as in the present work or in Ref. [13]. The dual character ($T = 3/2$ and $1/2$) of this state, possibly suggesting a large isospin mixing, is a long-standing problem and remained unsolved for a long time [33–36]. Recently, Fortune [37] made a reanalysis of the data in Ref. [33] and pointed out that the $1/2^+$ resonance could be much broader than previously considered. A complete understanding, including a theoretical prediction for the width, has still not been reached.

To form a $1/2^+$ resonance, the α particle must be coupled by $l = 1$ (p wave). Our R-matrix calculation shows that the sharp resonance could not be formed with a p wave, but an f-wave resonance fits our experimental excitation function perfectly.

Considering the above points, the present result suggests a different point of view: The resonance observed in this work may not be the known one at 12.56 MeV but may be another one located at 12.63 MeV having a different J^π. They might have been considered as the same resonance in some previous measurements, such as in Ref. [13]. The J^π of the state can be $3/2^+$, which was listed as a possible assignment in Ref. [33]. Another suggestion made by Soić *et al.* [22] was that this state can have a $J^\pi = 9/2^+$ from schematics of the rotational band of an α-cluster state, which will be discussed later. We mainly discuss these two cases $J^\pi = 3/2^+$ and $9/2^+$ below. $J^\pi = 5/2^+$ and $7/2^+$ are also possible assignments for this state from our measurements alone but are not supported by any previous studies.

R-matrix calculations for various combinations of J^π for this state and the next 13.03-MeV state are illustrated in Fig. 7, and the combinations of J^π considered are listed in Table II with the best-fit values of Γ_α. Case (a) shows the curve assuming $J^\pi = 1/2^+$ for 12.63 MeV, but it totally deviates from the experimental data. The conclusion is that both $J^\pi = 3/2^+$ and $9/2^+$ [cases (b) and (e)] are consistent with our data. For the $J^\pi = 3/2^+$ case, Γ_α is as large as the Wigner limit and is consistent with the previous value [18]. The width should be comparably smaller if we take $J^\pi = 9/2^+$. The other cases are discussed in the next subsection.

E. Resonance at 13.03 MeV

This resonance was observed initially via the ^{10}B$(n,\alpha)^7$Li reaction [38] and then via ^{7}Li + α inelastic scattering at 13.03 MeV [13]. Later, two states at 13.12 MeV ($J^\pi = 9/2^-$) and 13.17 MeV ($5/2^+$ or $7/2^+$) were introduced in the analysis

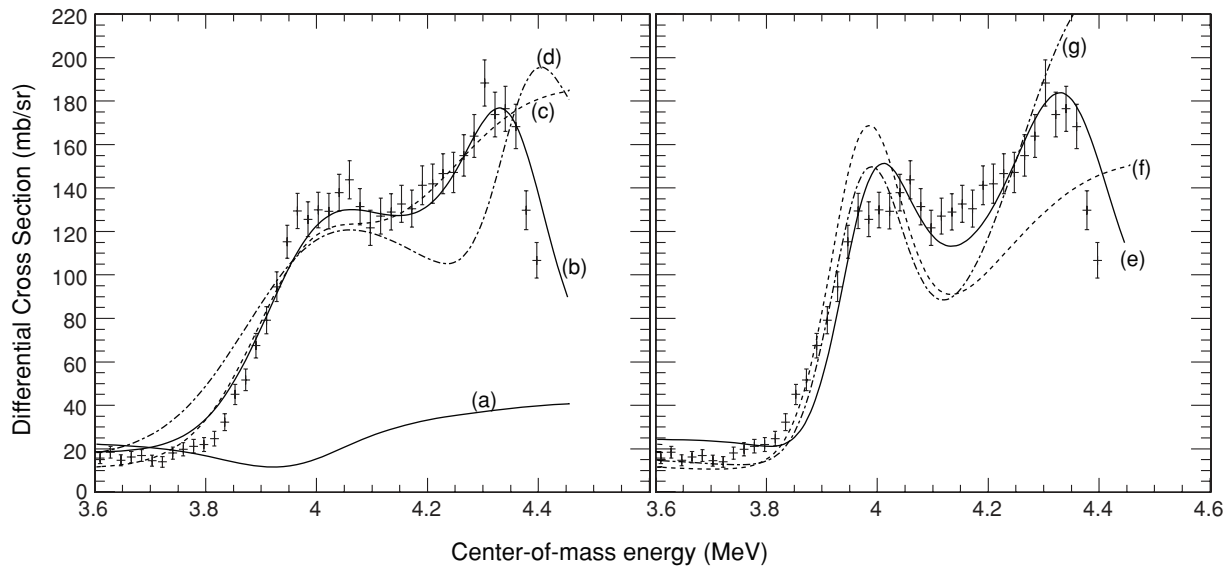

FIG. 7. High-energy part of the excitation function of ^{7}Li + α elastic scattering with calculations assuming several combinations of spin and parity, as in Table II. The best fit shown in Fig. 6 corresponds to case (b).

TABLE II. Combinations of J^π considered in the R-matrix fit shown in Fig. 7 and Γ_α obtained by the fit. Uncertainties are only shown for good fits. The last two rows show Γ_α for the other possible spin-parity combinations, but they are not supported by any previous studies.

Case	12.63 MeV		13.03 MeV	
	J^π	Γ_α (keV)	J^π	Γ_α (keV)
(a)	$1/2^+$	270	...	...
(b)	$3/2^+$	$270\ ^{-70}_{+100}$	$9/2^-$	$90\ ^{-30}_{+40}$
(c)	$3/2^+$	280	$5/2^+$	740
(d)	$3/2^+$	460	$7/2^+$	44
(e)	$9/2^+$	$42\ ^{-9}_{+11}$	$9/2^-$	$180\ ^{-40}_{+70}$
(f)	$9/2^+$	52	$5/2^+$	860
(g)	$9/2^+$	51	$7/2^+$	460
	$5/2^+$	$260\ ^{-100}_{+140}$	$9/2^-$	$150\ ^{-50}_{+80}$
	$7/2^+$	$80\ ^{-20}_{+30}$	$9/2^-$	$170\ ^{-40}_{+60}$

of Ref. [18], and the 13.03-MeV resonance was regarded as the former one [6]. Zwiegliński *et al.* [19] observed a state by the ^{9}Be(^{3}He,p)^{11}B reaction at 13.137 MeV, which is the value in the compilation [12] for the $J^\pi = 9/2^-$ state. However, obviously, there is some confusion regarding the energy and J^π of this level because they also mention that a state with $J^\pi = 9/2^-$ was not expected to be strongly excited by that reaction. After all, the assignment of $J^\pi = 9/2^-$ is not so evident since no measurement is known that observed this resonance separately from other ones and determined its J^π as $9/2^-$.

In the present analysis, we considered three possible J^π for the levels previously observed at 13.137 and 13.16 MeV: $9/2^-$, $5/2^+$, and $7/2^+$. A sudden fall in the spectrum at $E_{\rm cm} = 4.4$ MeV corresponds to the highest limit of the energy acceptance of our measurement. The two highest-energy points shown in Fig. 7 were excluded in the R-matrix fitting. The rest of the points, covering the peak cross section, were within the energy acceptance, and no considerable efficiency reduction is expected. For the cases of $J^\pi = 5/2^+$ and $7/2^+$ [cases (c), (d), (f), and (g)], the agreement of the experimental and calculated curves was worse than for cases (b) and (e), and the peak must be extended toward higher energy. However, this peak was observed with a sharp structure in Cusson's spectrum [13]. Therefore, we reject these two positive-parity cases and take $9/2^-$ as the J^π for this state.

A similar discussion could be applied for the cases when the 12.63-MeV state was assumed to have a spin parity of $J^\pi = 5/2^+$ or $7/2^+$, and the 13.03-MeV state should have a $J^\pi = 9/2^-$. The last two rows in Table II show Γ_α under such assumptions.

V. DISCUSSION

A. α cluster structure

As shown in Table I, we have observed several resonances with large Γ_α, comparable to the Wigner limit. The large Γ_α are consistent with a view that a component of an α-particle wave function often behaves as a cluster in the ^{11}B nucleus.

Rotational bands in ^{11}B, which might be related to the cluster structure, were previously discussed [22,39]. Several possible rotational bands in ^{11}B are shown in Fig. 8. In Ref. [39], the discussion was based on the Nilsson cranking model. The large moment of inertia $\Im$ in the positive-parity rotational band (indicated as $K = 5/2^+$ in Fig. 8), where $\hbar^2/2\Im = 0.25$ MeV, was considered to be due to strong deformation of the nucleus. A negative-parity band (negative band 1 in Fig. 8) was proposed, and the sudden increment of the moment of inertia at the $9/2^-$ state was also attributed to the deformation, consistent with their calculation. It might be curious that the $3/2^-$ (ground) and $1/2^-$ states were appearing in reversed energy in the proposed band. In the calculation [39], they found a level energy $3/2^-$ close to, but not lower than, that of $1/2^-$.

In Ref. [22], another positive-parity rotational band $K = 3/2^+$, where $\hbar^2/2\Im$ is 0.22 MeV, was also discussed, which is also shown in Fig. 8. In Fig. 8, we tentatively assumed the 12.63 MeV resonance has a J^π of $9/2^+$ and belongs to the $K = 3/2^+$ band.

In the present work, two negative-parity states at 10.34 MeV ($5/2^-$) and 13.03 MeV ($9/2^-$) were observed as strong resonances. These two negative-parity states, along with the

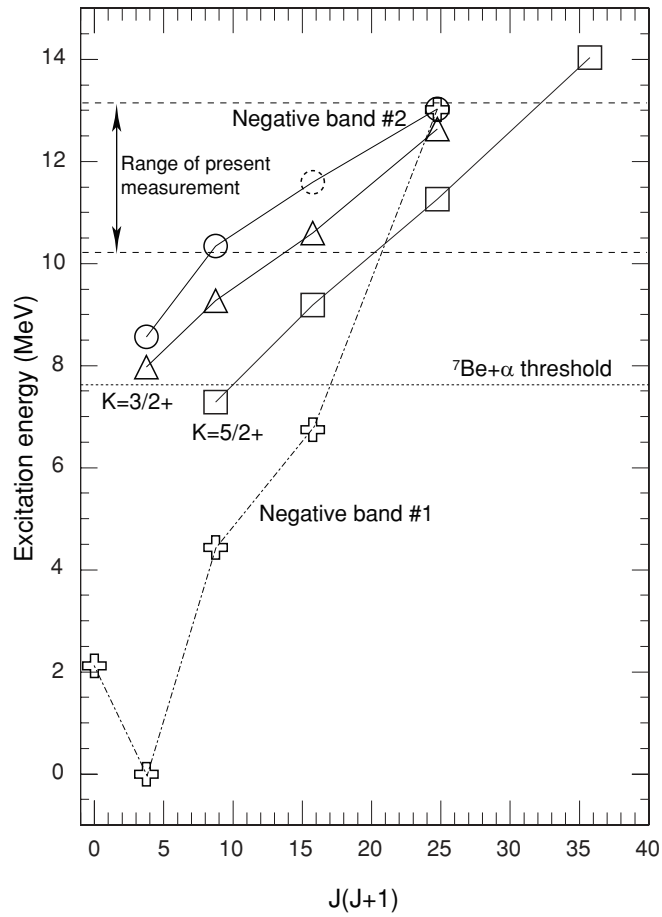

FIG. 8. Rotational bands in ^{11}B, showing that the excitation energy has a linear dependence on $J(J+1)$.

TABLE III. Parameters used in the reaction rate calculation. The dominant destination states of the γ decay according to a calculation are also shown. The uncertainties are only those from our Γ_α measurements.

Case	E_{ex} (MeV)	J^π	Γ_{tot} (keV)	Γ_α (keV)	Γ_γ (eV)	ω	$\omega\gamma$ (eV)	Dominant destination
(a)	11.29	$9/2^+$	110	35 ± 4	31	2.5	25 ± 3	6.74 MeV ($7/2^-$)
(b)	12.63	$3/2^+$	$270\ ^{-60}_{+100}$ [a]	$270\ ^{-70}_{+100}$	1.4×10^3	1.0	$(1.4\ ^{-0.1}_{+0}) \times 10^3$	ground ($3/2^-$)
(c)	12.63	$9/2^+$	210	$42\ ^{-9}_{+11}$	68	2.5	$34\ ^{-7}_{+9}$	6.74 MeV ($7/2^-$)
(d)	13.03	$9/2^-$	460	$140\ ^{-80}_{+110}$	26	2.5	$20\ ^{-12}_{+15}$	9.19 MeV ($7/2^+$)

[a] $\Gamma_{tot} = \Gamma_\alpha$ was assumed when our Γ_α exceeded known Γ_{tot}.

8.56-MeV state, may form a new band, shown as negative band 2 in Fig. 8. According to a recent calculation based on the antisymmetrized molecular dynamics (AMD) method [40,41], a negative-parity band may emerge above the ^{7}Li + α threshold. The band head is the 8.56-MeV ($3/2^-$) state, which is considered to be a dilute cluster state [1,3,4]. The calculation result suggests the band has sizable $E2$ transition strengths of 20–30 e^2 fm^4 between the neighboring member states. The calculated levels do not show an exact linear dependence on $J(J+1)$, and the band may not be interpreted as a simple rotational band. The small level spacing in the proposed band is consistent with the AMD calculation. If the 13.03 MeV ($9/2^-$) is a member of the new negative band 2 proposed here, the sudden change in the moment of inertia, assumed in negative band 1, may not be necessary. Note that the broad neutron-decaying resonance we introduced at 11.59 MeV has an energy and J^π exactly on the line (see dashed circle), although we do not simply regard this as a similar resonance belonging to the band.

The 12.56-MeV state was considered to be a candidate for the fully developed cluster-condensed state with $J^\pi = 1/2^+$ and $T = 1/2$ suggested by Yamada [5]. However, we observed no strong resonance having $J^\pi = 1/2^+$ and $T = 1/2$ at or around this energy. The resonance might be too weak to be observed with our method. The $J^\pi = 1/2^+$state should be expressed by a coupling of $\alpha + \alpha + t$ with $l = 0$, but ^{7}Li is primarily a coupling of α and t with $l = 1$. Consequently, the α and t in ^{7}Li must be decoupled by scattering with α to form such a state. Therefore, the probability to form the $J^\pi = 1/2^+$ state from the ^{7}Li + α channel ($J^\pi = 3/2^-$ and 0^+) might be small. More experimental evidence is required to confirm the existence of such a cluster-condensed state.

B. Reaction rate

The resonances observed in the present work might contribute to the astrophysical reaction rate of ^{7}Li$(\alpha,\gamma)^{11}$B at high temperature. Here we calculate the resonant reaction rate and compare it with the total reaction rate evaluated in Nuclear Astrophysics Compilation of Reaction Rates (NACRE) [42]. In the evaluation in NACRE, seven resonances up to $E_{ex} =$ 10.60 MeV are included. The resonant reaction rates $N_A\langle\sigma v\rangle_R$ were calculated for three resonances that we clearly observed at energies higher than 10.60 MeV, using the analytical formula described in Ref. [42]. As for the resonance at $E_{ex} = 12.63$ MeV, calculation results for J^π based on previous studies ($3/2^+$, $9/2^+$) are shown.

Table III shows the parameters we used in the calculation. Γ_α is known from our measurement. Since Γ_γ and the decay scheme were experimentally unknown for this energy range, we evaluated Γ_γ by a simple calculation based on the Weisskopf unit. We used the total widths Γ_{tot} in [12] or fixed at our Γ_α when it exceeded the total width in [12]. ω and $\omega\gamma$ are the statistical factor and the strength of the resonance, respectively. The uncertainties in $\omega\gamma$ that originated from our Γ_α measurements are also shown in Table III. However, the uncertainties in Γ_{tot} and Γ_γ, which are not known precisely, can be even larger than that of Γ_α.

The calculated contribution to the reaction rate is shown in Fig. 9 for each resonance separately. Cases (a)–(d) correspond to the ones in Table III. Cases (b) and (c) have the same resonance, but their magnitudes differ. The reason is that resonant state (b) can decay to the ground state directly with an $E1$ transition, but (c) cannot because of its high spin. As shown in Fig. 9, the only considerable contribution from the resonance of case (b) occurs in the very high temperature region, $T_9 > 5$. Considering that the Weisskopf unit tends to overestimate the width in such cases, the contribution for the other high-spin resonances are likely to make no significant contribution to the reaction rate even at $T_9 = 10$. However, studies on the γ widths and decay scheme and determination of J^π are needed for a conclusive evaluation of the reaction rate.

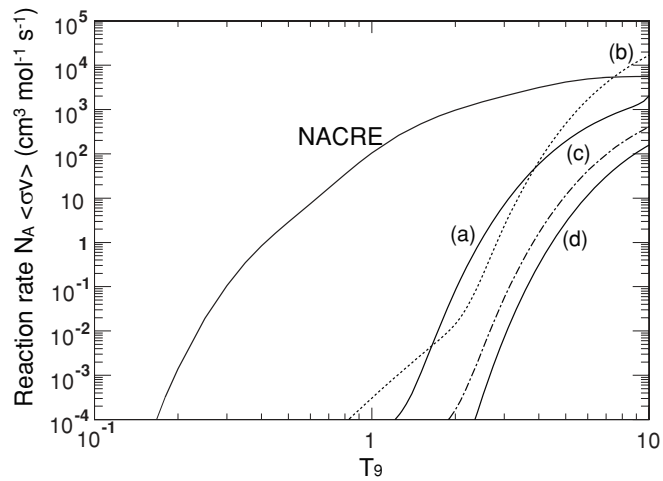

FIG. 9. Resonant reaction rate of ^{7}Li(α,γ) for 11.29, 12.63, and 13.03 MeV resonances, calculated by the analytical formula. The total reaction rate evaluated by NACRE is also shown for comparison. T_9 is the temperature in GK.

VI. SUMMARY

We have studied α resonant scattering of ^{7}Li at CRIB. We measured the excitation functions for cross sections of the $^7\mathrm{Li} + \alpha$ elastic and inelastic scatterings and the $^7\mathrm{Li}(\alpha, p)$ reaction up to $E_{\mathrm{ex}} = 13.1$ MeV ($E_{\mathrm{cm}} = 4.4$ MeV) using the thick-target method in inverse kinematics. The excitation function of the elastic scattering exhibited resonances mostly consistent with previous measurements, and we successfully determined their resonance parameters. In particular, a reliable determination for α decay widths was made for the first time. A $J^\pi = 1/2^+$ and $T = 3/2$ resonance was known to be at 12.56 MeV, but we proposed the existence of another $T = 1/2$ resonance at 12.63 MeV, for which J^π is possibly $3/2^+$ or $9/2^+$. ^{11}B is known to have rotational bands with a large moment of inertia. We proposed a new negative-parity band consistent with a theoretical calculation, but its character (e.g., rotational or not) should be studied in more detail in the future. We evaluated the resonant reaction rate of $^7\mathrm{Li}(\alpha,\gamma)^{11}$B at high temperature using the new α widths, but a major enhancement over the evaluation by NACRE is not expected for $T_9 < 5$.

ACKNOWLEDGMENTS

The experiment was performed at RI Beam Factory operated by RIKEN Nishina Center and CNS, University of Tokyo. We are grateful to the RIKEN and CNS accelerator staff for their help. We truly appreciate the useful discussions and suggestions of Professor Y. K. En'yo and Mr. T. Suhara based on their latest theoretical calculations. This work was partly supported by JSPS KAKENHI No. 21340053 and the Grant-in-Aid for the Global COE Program "The Next Generation of Physics, Spun from Universality and Emergence" from the Ministry of Education, Culture, Sports, Science and Technology (MEXT) of Japan.

[1] Y. Kanada En'yo, Phys. Rev. C **75**, 024302 (2007).
[2] A. Tohsaki, H. Horiuchi, P. Schuck, and G. Röpke, Phys. Rev. Lett. **87**, 192501 (2001).
[3] T. Kawabata, H. Akimune, H. Fujimura, H. Fujita, Y. Fujita, M. Fujiwara, K. Hara, K. Y. Hara, K. Hatanaka, T. Ishikawa *et al.*, Phys. Rev. C **70**, 034318 (2004).
[4] T. Kawabata, H. Akimune, H. Fujita, Y. Fujita, M. Fujiwara, K. Hara, K. Hatanaka, M. Itoh, Y. Kanada-En'yo, S. Kishi *et al.*, Phys. Lett. B **646**, 6 (2007).
[5] T. Yamada and Y. Funaki, Phys. Rev. C **82**, 064315 (2010).
[6] F. Ajzenberg-Selove, Nucl. Phys. A **506**, 1 (1990).
[7] D. Tilley, J. Kelley, J. Godwin, D. J. Millener, J. E. Purcell, C. G. Sheu, and H. R. Weller, Nucl. Phys. A **745**, 155 (2004).
[8] T. Yoshida, T. Kajino, H. Yokomakura, K. Kimura, A. Takamura, and D. H. Hartmann, Phys. Rev. Lett. **96**, 091101 (2006).
[9] P. Paul, N. Puttaswamy, and D. Kohler, Phys. Rev. **164**, 1332 (1967).
[10] G. Hardie, B. W. Filippone, A. J. Elwyn, M. Wiescher, and R. E. Segel, Phys. Rev. C **29**, 1199 (1984).
[11] G. Gyürky, Z. Fülöp, E. Somorjai, G. Kiss, and C. Rolfs, Eur. Phys. J. A **21**, 355 (2004).
[12] F. Ajzenberg-Selove, Nucl. Phys. A **506**, 1 (1990).
[13] R. Cusson, Nucl. Phys. **86**, 481 (1966).
[14] H. Bohlen, N. Marquardt, W. von Oertzen, and P. Gorodetzky, Nucl. Phys. A **179**, 504 (1972).
[15] R. Jambunathan and R. Hobbie, Phys. Rev. **172**, 1065 (1968).
[16] R. Lane, S. Hausladen, J. Monahan, A. Elwyn, F. Mooring, and J. A. Langsdorf, Phys. Rev. C **4**, 380 (1971).
[17] G. Schmidt, J. Mösner, and J. Schintlmeister, Nucl. Phys. A **173**, 449 (1971).
[18] S. Hausladen, C. Nelson, and R. Lane, Nucl. Phys. A **217**, 563 (1973).
[19] B. Zwiegliński, W. Benenson, G. Crawley, S. Galès, and D. Weber, Nucl. Phys. A **389**, 301 (1982).
[20] R. Aryaeinejad, W. Falk, N. Davison, J. Knudson, and J. Campbell, Nucl. Phys. A **436**, 1 (1985).
[21] N. R. Fletcher, D. D. Caussyn, F. Maréchal, N. Curtis, and J. A. Liendo, Phys. Rev. C **68**, 024316 (2003).
[22] N. Soić, M. Freer, L. Donadille, N. Clarke, P. Leask, W. Catford, K. Jones, D. Mahboub, B. Fulton, B. Greenhalgh *et al.*, Nucl. Phys. A **742**, 271 (2004).
[23] S. Kubono, Y. Yanagisawa, T. Teranishi, S. Kato, T. Kishida, S. Michimasa, Y. Ohshiro, S. Shimoura, K. Ue, S. Watanabe *et al.*, Eur. Phys. J. A **13**, 217 (2002).
[24] Y. Yanagisawa, S. Kubono, T. Teranishi, K. Ue, S. Michimasa, M. Notani, J. J. He, Y. Ohshiro, S. Shimoura, S. Watanabe *et al.*, Nucl. Instrum. Methods Phys. Res., Sect. A **539**, 74 (2005).
[25] K. P. Artemov, O. P. Belyanin, A. L. Vetoshkin, R. Wolskj, M. S. Golovkov, V. Z. Gol'dberg, M. Madeja, V. V. Pankratov, I. N. Serikov, V. A. Timofeev *et al.* Sov. J. Nucl. Phys. **52**, 408 (1990).
[26] J. Ziegler, J. Biersack, and M. Ziegler, *SRIM: The Stopping and Range of Ions in Matter* (Lulu Press, Morrisville, NC, 2008).
[27] C. Li and R. Sherr, Phys. Rev. **96**, 389 (1954).
[28] M. Konstantinova, E. Myakinin, A. Petrov, and A. Romanov, Sov. J. Exp. Theor. Phys. **16**, 278 (1963).
[29] N. Larson, Oak Ridge National Laboratory Report No. ORNL/TM-9179/R5, 2000 (unpublished).
[30] H. G. Bingham, K. W. Kemper, and N. R. Fletcher, Nucl. Phys. A **175**, 374 (1971).
[31] D. Groce, J. McNally, and W. Whaling, Bull. Am. Phys. Soc. **8**, 486 (1963).
[32] B. Watson, C. Chang, and M. Hasinoff, Nucl. Phys. A **173**, 634 (1971).
[33] D. Goosman, E. Adelberger, and K. Snover, Phys. Rev. C **1**, 123 (1970).
[34] R. Sherr and G. Bertsch, Phys. Rev. C **32**, 1809 (1985).
[35] R. Sherr and H. T. Fortune, Phys. Rev. C **64**, 064307 (2001).
[36] F. C. Barker, Phys. Rev. C **69**, 024310 (2004).
[37] H. T. Fortune, Phys. Rev. C **74**, 034328 (2006).

[38] B. Petree, C. Johnson, and D. Muller, Phys. Rev. **83**, 1148 (1951).
[39] I. Ragnarsson, S. Åberg, H.-B. Håkansson, and R. Sheline, Nucl. Phys. A **361**, 1 (1981).
[40] T. Suhara and Y. Kanada En'yo, Prog. Theor. Phys. **123**, 303 (2010).
[41] T. Suhara and Y. Kanada En'yo (private communication, 2010).
[42] C. Angulo *et al.*, Nucl. Phys. A **656**, 3 (1999).